Wave Motion 68 (2017) 210–217

Contents lists available at ScienceDirect

Wave Motion

journal homepage: www.elsevier.com/locate/wavemoti

Three-dimensional overturned traveling water waves

Benjamin F. Akers *, Jonah A. Reeger

Department of Mathematics and Statistics, Air Force Institute of Technology, Dayton, OH, United States

HIGHLIGHTS

- A system of equations for traveling waves on parameterized surfaces is developed.
- Three dimensional traveling waves are computed via numerical continuation.
- An example of a three-dimensional traveling wave with overturned crests is presented.
- The structure of dimension-breaking bifurcations is investigated.

ARTICLE INFO

Article history:
Received 11 May 2016
Received in revised form 4 October 2016
Accepted 9 October 2016
Available online 21 October 2016

Keywords:
Overturning
Traveling waves
Gravity-capillary
Dimension-breaking

ABSTRACT

Traveling gravity-capillary water waves on the interface of a three-dimensional fluid of infinite depth are computed. The vortex sheet formulation with the small scale approximation is used as the mathematical model for the fluid motion. The fluid interface is parameterized isothermally. The traveling wave ansatz for parameterized surfaces is described. Waves are computed using Fourier collocation and quasi-Newton iteration; large amplitude overturned traveling waves are computed via a dimension-breaking based numerical continuation method.

Published by Elsevier B.V.

1. Introduction

We study periodic waves of the interface between two constant-density fluids undergoing irrotational motions. The fluid regions are infinitely deep in the vertical direction and periodic in the horizontal direction. We seek traveling wave solutions, in which the free surface is of permanent form and steadily translating. This study is fundamentally concerned with waves on a two-dimensional interface, between three-dimensional fluids, which may have overhanging crests (or troughs).

It is the understanding of the authors that no study has been conducted for fully three-dimensional water waves which are both overturned and traveling. A number of studies have considered overturning in the time dependent problem, for example [1–7] with a review in [8]. There are also numerous computations of permanent three-dimensional waves (both traveling and standing waves) in which the interface is parameterized by the horizontal coordinates, for example [9–14]. There have been studies of axisymmetric three-dimensional overturned traveling waves in fluid jets, where such symmetry is natural [15–17].

The reasons for the absence of previous work on three-dimensional overturned traveling waves are two-fold. First, one must have a three-dimensional formulation of the problem which allows for traveling waves which are overturning. Conformal mappings are by far the most popular technique for the two-dimensional problem, but do not generalize to three-dimensions. In a recent work, the first author and collaborators have developed a formulation which extends to three-dimensions and allows for the computation of traveling waves on interfaces with arbitrary parameterizations [18]. It is in

* Corresponding author.
E-mail address: Benjamin.Akers@afit.edu (B.F. Akers).

http://dx.doi.org/10.1016/j.wavemoti.2016.10.001
0165-2125/Published by Elsevier B.V.

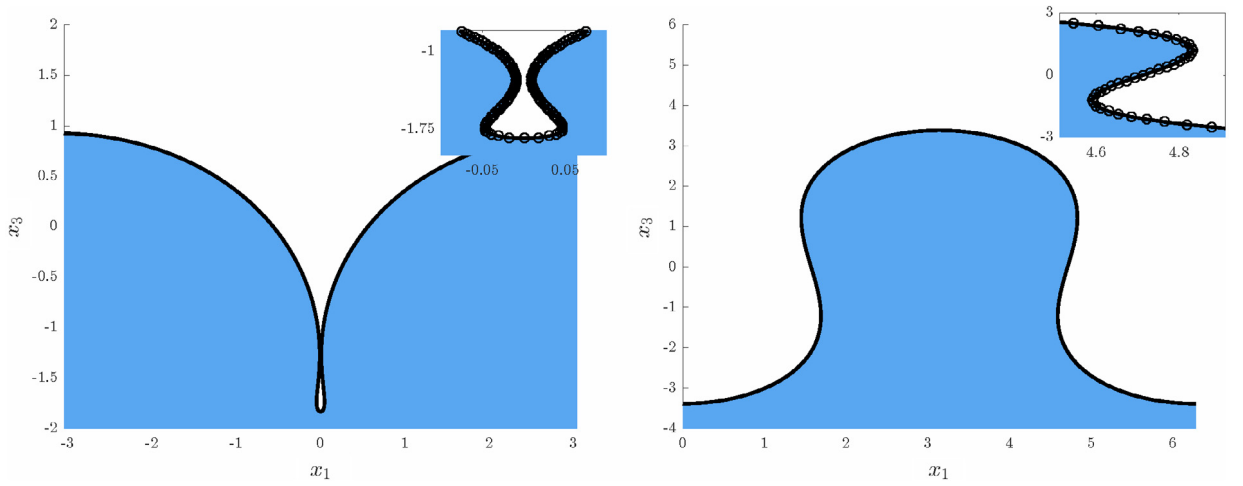

Fig. 1.1. The extreme water wave on branches of traveling waves at two different Bond numbers in a two-dimensional fluid are depicted. Left: The large amplitude limit of traveling waves with $\sigma = 1/8$ is a self-intersecting profile. Right: The steepest wave for $\sigma = -1/10$. The left panel was computed with $M_a = 512$ points, the right panel with $M_a = 128$. The increased resolution on the left is to resolve the extreme curvature within the bubble. In both panels the inset figures show close-ups of the overturned portion of the wave, with grid-points marked with circles.

this formulation that this paper proceeds to three-dimensions. The need for such parametric formulations of the water wave problem is not unknown. Alternative to the track taken here, Bridges and Dias proposed a Hamiltonian formulation which allows for arbitrary interface parameterizations [19].

The second reason for the lack of computations of overhanging three-dimensional traveling waves is the extreme expense of the computation itself, as will be discussed explicitly here, and is reviewed in [8]. In this work, the extreme cost will be partially ameliorated via the use of an approximate model, called the small-scale approximation, proposed in [20] and later used in [21]. The approximation allows the most costly part of the computation, the evaluation of the Birkhoff–Rott integral, to be computed via fast Fourier transforms. The small scale approximation, although exact in the small-amplitude limit, is not based on a small-amplitude assumption, and will be used here to compute large amplitude three-dimensional traveling waves, including those with overturned crests and troughs.

For two-dimensional fluids, a significant amount of work has been done in the study of both dynamic and steady overturned waves. We will not try to review them all here. Most relevant to this work are the exact traveling solutions of Crapper [22] and the numerically computed waves of Meiron and Saffman [23], as these two waves are qualitatively similar to the cross-sections of the three-dimensional waves computed here. This paper also is an outgrowth of a number of recent two-dimensional studies by one of the authors. The traveling wave ansatz developed in [18] has since been used extensively to compute two-dimensional overturning traveling waves [24,25].

The remainder of the paper is organized as follows. In Section 2 we present the vortex sheet formulation of the potential flow equations, the small scale approximation to the Birkhoff–Rott equations, and the traveling wave ansatz. These three ingredients combine to give the system of equations which are solved for three-dimensional traveling waves. In Section 3 we present the numerical procedure used to compute traveling waves as well as the numerical results. This Section 3 includes an example of an overturned three-dimensional traveling wave and discussion of the dimension-breaking continuation procedure used to compute three-dimensional waves. In Section 4 we summarize our results and present future research avenues.

2. Formulation

In this work we compute three-dimensional traveling waves in a model for the interface between two-fluids. In particular, we are interested in the case where the fluid interface is overturned, that is, where the vertical displacement is not a function of horizontal Cartesian coordinates. To compute such three-dimensional overturning waves, we will represent the interface as a parameterized surface $\vec{X}(\alpha, \beta, t) = (x_1(\alpha, \beta, t), x_2(\alpha, \beta, t), x_3(\alpha, \beta, t))$. Following Ambrose, Siegel and Tlupova, [1], we will enforce that this parameterization is isothermal, i.e. that

$$\vec{X}_\alpha \cdot \vec{X}_\beta = 0, \quad \text{and} \quad G \equiv \|\vec{X}_\alpha\|^2 = \lambda \|\vec{X}_\beta\|^2 \equiv \lambda E \tag{2.1}$$

with

$$\lambda = \frac{\int\int G \, d\alpha d\beta}{\int\int E \, d\alpha d\beta}.$$

We will think of λ as a constant specified at the beginning, describing the aspect ratio of the parameterization (or how much longer the wave is in α than in β). We choose to set $\lambda = 1$, so that $G = E$. We set the ranges for α and β to be equal to the

period of the wave in the corresponding horizontal coordinates, that is

$$x_1(\alpha + P_1, \beta) = x_1(\alpha, \beta) + P_1, \quad \text{and} \quad x_2(\alpha, \beta + P_2) = x_2(\alpha, \beta) + P_2.$$

Numerically we will take $x_1 = \alpha + \tilde{x}_1$ and $x_2 = \beta + \tilde{x}_2$ where the $\tilde{x}_j$ are periodic corrections, which are more amenable to our Fourier-collocation based numerical method.

Useful in this parameterization are the second fundamental forms

$$L = \vec{X}_{\alpha,\alpha} \cdot \hat{\mathbf{n}}, \quad \text{and} \quad N = \vec{X}_{\beta,\beta} \cdot \hat{\mathbf{n}}.$$

In terms of which the mean curvature can be expressed as

$$\kappa = \frac{L\lambda + N}{2\lambda E}.$$

The isothermal parameterization is the three-dimensional analogy to the arclength parameterization used in [18,24]. The fluid velocity, $\vec{W}$, is given in terms of a Birkhoff–Rott integral,

$$\vec{W}(\vec{X}) = \frac{1}{4\pi} \sum_{n\in\mathbb{Z}} \sum_{m\in\mathbb{Z}} P.V. \iint (\mu'_\alpha \vec{X}'_\beta - \mu'_\beta \vec{X}'_\alpha) \frac{(\vec{X} - \vec{X}' - nP_1\mathbf{e_1} - mP_2\mathbf{e_2})}{\left|\vec{X} - \vec{X}' - nP_1\mathbf{e_1} - mP_2\mathbf{e_2}\right|^3} \, d\alpha' \, d\beta' \tag{2.2}$$

in which all the primed quantities are evaluated at (α', β'). The parameter P_1 is the period of the wave in the first horizontal coordinate, x_1, and P_2 is the period of the wave in the second horizontal coordinate, x_2. This integral is notoriously difficult to simulate, see [1], and will here be replaced by the small scale approximation of [20,21]. This approximation takes

$$W \approx \frac{1}{2} H_\alpha \left[\frac{\mu_\alpha X_\beta \times X_\alpha}{E^{\frac{3}{2}}} \right] - \frac{1}{2} H_\beta \left[\frac{\mu_\beta X_\alpha \times X_\beta}{E^{\frac{3}{2}}} \right]$$

which captures the near-singular behavior of the integral and avoids the significant difficulties associated with computing the Birkhoff–Rott integral, see, for example, Beale's discussion of the convergence of this integral [26]. The operators H_α and H_β are the Riesz transforms. The Riesz transforms are diagonalized by the Fourier transform, and have multiplicative Fourier symbols,

$$\widehat{H_\alpha f}(\mathbf{k}) = -i \frac{k_1}{\sqrt{k_1^2 + k_2^2}} \hat{f}, \quad \text{and} \quad \widehat{H_\beta f}(\mathbf{k}) = -i \frac{k_2}{\sqrt{k_1^2 + k_2^2}} \hat{f}.$$

The k_i are the components of the Fourier wave vector $\vec{k}$. One can also express the Riesz transforms in terms of differential operators as

$$H_\alpha = -\partial_\alpha \left(-\partial_\alpha^2 - \partial_\beta^2\right)^{-1/2} \quad \text{and} \quad H_\beta = -\partial_\beta \left(-\partial_\alpha^2 - \partial_\beta^2\right)^{-1/2}.$$

A study of the overturning waves with the full Birkhoff–Rott integral using the algorithm of Siegel and colleagues [1] is being pursued separately.

The Bernoulli equation for the evolution of the vortex sheet strength is

$$\begin{aligned} \mu_t \; = \; & \tau\kappa + \left(\frac{\mu_\alpha}{\sqrt{E}} (V_1 - W \cdot \hat{\mathbf{t}}_\mathbf{1}) + \frac{\mu_\beta}{\sqrt{E}} (V_2 - W \cdot \hat{\mathbf{t}}_\mathbf{2}) \right) \\ & + At \left(|W|^2 + 2W \cdot \hat{\mathbf{t}}_\mathbf{1} (V_1 - W \cdot \hat{\mathbf{t}}_\mathbf{1}) + 2W \cdot \hat{\mathbf{t}}_\mathbf{2} (V_2 - W \cdot \hat{\mathbf{t}}_\mathbf{2}) - \frac{\mu_\alpha^2 + \mu_\beta^2}{4E} - g x_3 \right). \end{aligned} \tag{2.3}$$

This equation is presented for a parameterization with $\lambda = 1$, so that $G = E$. Here V_j are the tangential components of the velocity of the interface in our parameterization, not to be confused with $W \cdot \hat{\mathbf{t}}_\mathbf{j}$, the velocity of fluid particles on the interface. The parameter τ is the surface tension coefficient, g is gravity, and $\text{At} = \frac{\rho_1 - \rho_2}{\rho_1 + \rho_2}$ is the Atwood ratio, comparing the densities of the upper and lower fluids with densities of $\rho_2 \rho_1$, respectively.

The kinematic equation for the interface is

$$\vec{X}_t = U\hat{\mathbf{n}} + V_1 \hat{\mathbf{t}}_\mathbf{1} + V_2 \hat{\mathbf{t}}_\mathbf{2} \tag{2.4}$$

where U is the physical normal velocity to the interface and V_j are chosen to preserve the isothermal parameterization. For a general interface motion, to preserve an isothermal parameterization requires that the V_j solve an elliptic equation, as discussed in [1]. For steadily translating interfaces, as is the case for traveling waves, the V_j can be determined by the kinematic condition (2.4) coupled with the prescription that the interface is traveling in the x_1-direction, $X_t = (c, 0, 0)$, yielding

$$\begin{pmatrix} c \\ 0 \\ 0 \end{pmatrix} = \begin{pmatrix} \hat{\mathbf{n}} & \hat{\mathbf{t}}_\mathbf{1} & \hat{\mathbf{t}}_\mathbf{2} \end{pmatrix} \begin{pmatrix} U \\ V_1 \\ V_2 \end{pmatrix}.$$

If one considers the speed c, and interface location $\mathbf{X}$ to be known, then U and V_j are specified

$$V_j = c(\hat{\mathbf{t}}_\mathbf{j})_1, \quad \text{and} \quad U = c(\hat{\mathbf{n}})_1. \tag{2.5}$$

The notation $(\hat{\mathbf{t}}_\mathbf{j})_i$ refers to the ith entry of tangent vector j.

From the perspective of the kinematic equation, any interface shape is allowable, so long as the velocity of the interface is coupled to the shape by (2.5). If one chooses, as we will here, to parameterize in a frame moving with the wave, then the interface shape is independent of time. A sufficient condition for traveling waves in such a frame is that the vortex sheet strength has $\mu_t = 0$. The coupling of $\mu_t = 0$ and (2.5), play the role of the traveling wave ansatz in this formulation. Combining this ansatz with Eq. (2.3) under an isothermal parameterization gives the equations for traveling waves.

To compute a traveling wave requires finding four functions x_1, x_2, x_3, and μ as well as a speed c, which solve four equations,

$$0 = \tau\kappa + \frac{1}{\sqrt{E}}(\tilde{\mathbf{V}} \cdot \nabla)\mu + \mathrm{At}\left(|W|^2 + 2W \cdot \hat{\mathbf{t}}_\mathbf{1}\tilde{V}_1 + 2W \cdot \hat{\mathbf{t}}_\mathbf{2}\tilde{V}_2 - \frac{1}{4E}|\nabla\mu|^2 - gx_3\right), \tag{2.6a}$$

$$0 = c(\hat{\mathbf{n}})_1 - W \cdot \hat{\mathbf{n}}, \tag{2.6b}$$

$$0 = X_\alpha \cdot X_\beta, \tag{2.6c}$$

$$0 = G - \lambda E, \tag{2.6d}$$

in which $\tilde{V}_j = c(\hat{\mathbf{t}}_\mathbf{j})_1 - W \cdot \hat{\mathbf{t}}_\mathbf{j}$, and $\tilde{\mathbf{V}} = (\tilde{V}_1, \tilde{V}_2)$. We append another equation fixing the wave amplitude to close the system. The measure of wave amplitude will vary in our numerical method. For the results in the following section we alternately use the crest height, total displacement, and the amplitude of a Fourier mode of the third coordinate.

3. Results and discussion

The numerical method used is a combination of Fourier collocation and a quasi-Newton iteration, similar to those used in [18,27,28]. The unknown functions x_1, x_2, x_3, and μ are all real functions of two parametric variables α and β. We compute both planar waves, which are constant in the direction transverse to propagation, and fully three-dimensional waves, which depend non-trivially on both α and β.

To compute overturned fully three-dimensional waves, we use a dimension-breaking approach. First a branch of traveling planar waves (trivial dependence in β) are computed. Because these waves do not depend on β, one needs only to compute the profile at a single location. This dimension reduction makes computing large amplitude planar waves significantly less expensive than computing fully three-dimensional branches of traveling waves. Next, branches of waves with non-trivial β dependence are computed as bifurcations from the branch of planar waves. These waves have transverse (β direction) periodicity which depends on the amplitude from which they bifurcate. The numerical cost to compute such waves is significantly greater than the planar waves; however, since one can pay the planar cost to reach large amplitude, we are able to compute well resolved, large amplitude, overturned, fully three-dimensional waves. An example of the dimension breaking bifurcation is depicted in Fig. 3.1.

The fully three-dimensional Fourier collocation begins with M_a points in α and M_b points in β, where $(\alpha, \beta) \in \left[-\frac{1}{2}P_1, \frac{1}{2}P_1\right) \times \left[-\frac{1}{2}P_2, \frac{1}{2}P_2\right)$. Thus direct projection of the these functions onto Fourier modes would yield $4M_aM_b$ unknowns. Problem symmetries allow for this number to be reduced significantly.

The number of unknowns are reduced via the folllowing sequence of arguments. The solutions sought are real functions, therefore one needs only compute the Fourier coefficients in one quadrant of Fourier space. Second, symmetries allow for one to look for $x_3(\alpha, \beta)$ which is doubly even (in both α and β) and $\mu(\alpha, \beta)$ which is odd in α and even in β. Similarly we seek $x_1(\alpha, \beta)$ which is odd in β and even in α, and $x_2(\alpha, \beta)$ which is even in α and odd in β. The last two are simply choices of how the parametric variables α and β are aligned with respect to the horizontal coordinates x_1 and x_2. These parity choices allow one to compute Fourier coefficients which are either pure real (if the function is even in both variables) or pure imaginary (if the function is even in one variable and odd in the other). Many of the spatial averages of these functions need not be solved for; odd functions have zero spatial means. The end result is that to compute a traveling wave one must solve for $M_aM_b - M_b - \frac{1}{2}M_a + 1$ Fourier coefficients (as well as the speed c).

The system of equations we solve are the projection of Eqs. (2.6) into Fourier space. For $(\mathbf{x}, \mu)$ with the above described parity, the equations support similar symmetries and give the same number of non-trivial Fourier coefficients as the equations. We couple to this system an equation specifying the size of the traveling wave to close the system. This last equation is used as our continuation parameter, the choice of which will vary along a branch of traveling waves. For small amplitude we use the total displacement $h = \max(x_3) - \min(x_3)$. For large amplitude we sometimes observe turning points, where the branch has a locally maximal displacement, in which case we switch to another measure of the wave size, for example a Fourier coefficient of x_3.

The primary numerical cost in computing traveling waves is the filling (and storing) of the approximation of the Jacobian in the quasi-Newton solver. We ameliorate this to some extent via Broyden's update [29], and by re-using Jacobian's during the continuation procedure. This does not avoid the expense of storing large Jacobian matrices. The highest resolution wave

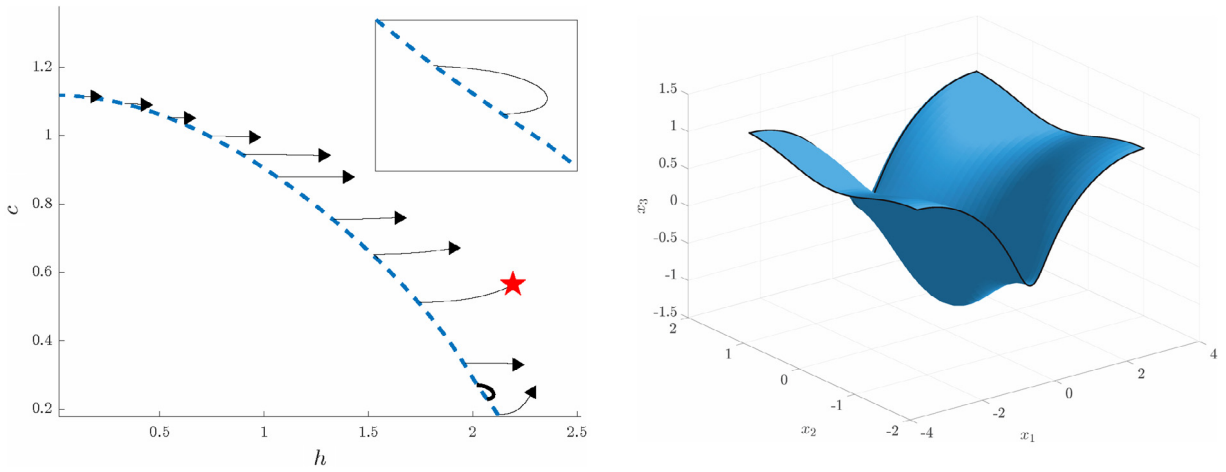

Fig. 3.1. The dimension breaking bifurcation of traveling waves solutions to Eqs. (2.6) is depicted in the speed, c, and total displacement, $h = \max(z) - \min(z)$, plane. The waves bifurcate from a planar wave with Bond number $\sigma = 1/8$, whose speed–amplitude curve is marked with the dashed curve in the left panel. The secondary, dimension-breaking bifurcations occur at different amplitudes depending on the transverse period (the secondary bifurcation's speed–amplitude curves are marked with arrows at their tips). Notice that there is closed loop, representing a "return to trivial" global bifurcation, a close-up of this loop is inset. An example genuinely three-dimensional profile, marked with the star in the left panel, is depicted in the right panel.

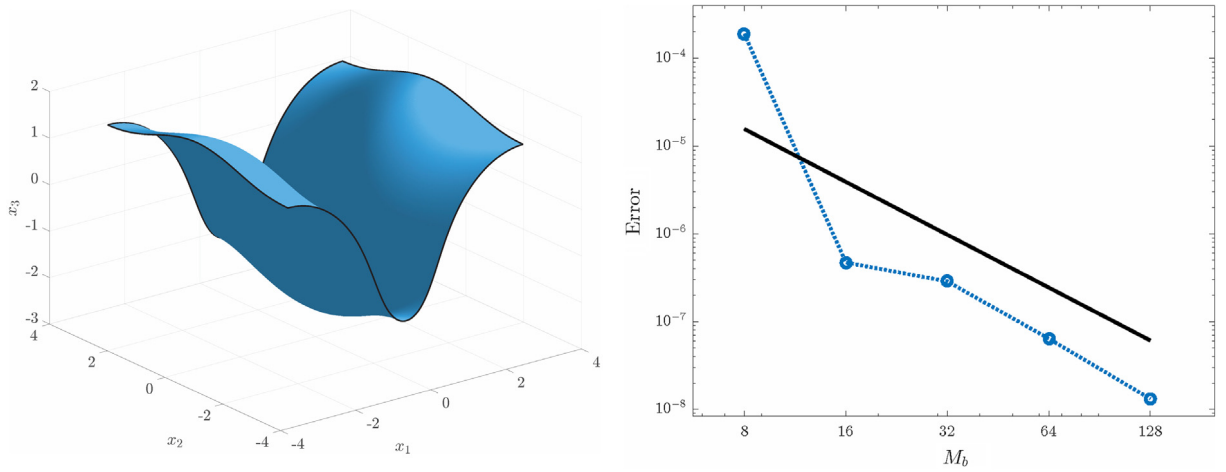

Fig. 3.2. **Left**: A relatively large amplitude wave, $h = 4.23$, used for the convergence study on the right. This wave has At $= 1$, $g = -0.1$, $\tau = 2$. At larger amplitude and transverse variation this wave overturns, and is depicted in Fig. 3.4. **Right**: The Cauchy error of the computed wave speed, $|c(M_b) - c(2M_b)|$, is plotted as a function of points in the β coordinate M_b (marked with circles). The number of points in the α direction is fixed at $M_a = 256$. The solid line is $O(M_b^{-2})$.

computed had $M_a = 128$ and $M_b = 256$; at this resolution the Jacobian is $32\,450 \times 32\,450$, which in IEEE type double costs 8.4 GB just to store. Rather than push the computational limits of our machine, we have chosen to present only waves which are very regular. This allows for highly resolved computations at a relatively small number of points (see Fig. 3.4, which has $M_a = 128$, $M_b = 32$). The computations done at this resolution are numerically exact at small amplitude, and have errors smaller than visible graphically at large amplitude. Fig. 3.2 presents evidence of the convergence of the numerical method at relatively large amplitude.

For this first work on overturned traveling waves, the small-scale approximation to the Birkhoff–Rott integral is employed. This reduces the cost of computing W to $O(M_a M_b \log(M_a M_b))$. Simulation of the full Birkhoff–Rott integral is possible, but significantly more complicated, and is being pursued separately. The difficulty of simulating the Birkhoff–Rott integral for three-dimensional fluids is well known [11]. A modern fast technique is that of Siegel and colleagues [1] which combines Ewald summation, matched near-field and far field expansions and a tree code, in the spirit of the "Fast Multipole Method" [5,30].

The computations here are based on a quasi-Newton iteration, thus they require initial guesses. For small amplitude, it is natural to use a Stokes' expansion to compute one traveling wave, and then compute larger amplitude waves via numerical continuation. This approach is numerically costly, as one must pay the cost of computing a fully three-dimensional wave at every amplitude along the branch of traveling waves. We take an alternate tactic, following dimension breaking bifurcations from a planar (two-dimensional) traveling wave.

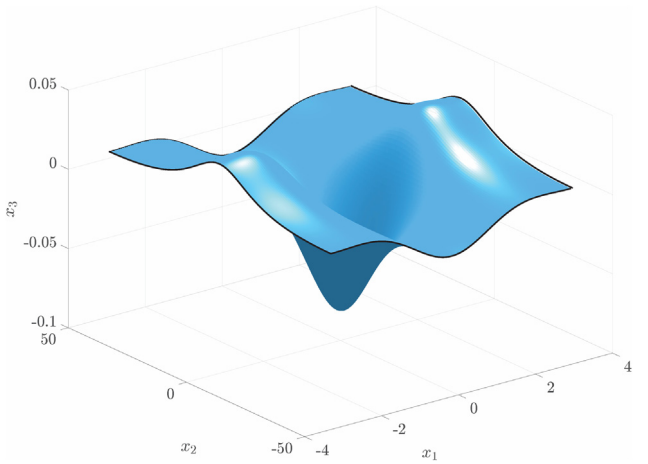

Fig. 3.3. A three-dimensional traveling wave which bifurcates from a planar wave at small amplitude. As is typical for small amplitude planar waves, the transverse period of the three-dimensional bifurcation is large, here $P_2 = 30\pi$, where $P_1 = 2\pi$. This wave was computed with At $= 1$, $\tau = 2$, $g = 2$, with $M_a = 128$ and $M_b = 256$.

To compute three-dimensional bifurcations from a planar wave, our computations begin with a planar solution

$$x_1 = \tilde{x}_1(\alpha), \qquad x_2 = \beta, \qquad x_3 = \tilde{x}_3(\alpha), \quad \text{and} \quad \mu = \tilde{\mu}(\alpha). \tag{3.1}$$

A small spatial variation in the transverse direction is then added to the planar solution, and the perturbed wave is used as an initial guess for three-dimensional traveling wave. The initial guesses used here are exactly the planar solutions in the x_1 and x_2 coordinates, from (3.1). For the displacement and vortex sheet strength, we add small transverse dependence of period P_2,

$$x_3 = \tilde{x}_3(\alpha)\left(1 + \delta\cos\left(\frac{2\pi}{P_2}\beta\right)\right), \quad \text{and} \quad \mu = \tilde{\mu}(\alpha)\left(1 + \delta\cos\left(\frac{2\pi}{P_2}\beta\right)\right). \tag{3.2}$$

In (3.2) the parameter δ is a small constant, we used $\delta = 0.005$. The ansatz (3.2) is not always close to a genuinely three-dimensional traveling wave. We observe a single period at each displacement of planar waves $P_2 = P_2(h)$ for which (3.2) approximates a three-dimensional wave. In order to find dimension breaking bifurcations one must guess one such period, along with all the other unknowns. After a successful guess, continuation is used to find larger amplitude, fully three-dimensional waves.

A significant challenge in this procedure is guessing the transverse period, P_2, at which the bifurcations occur. We observed that the periods are largest at small amplitude. In Fig. 3.1, we present a branch of planar waves, and a sequence of dimension-breaking bifurcations. Each of these secondary bifurcations have their own transverse period, and appear as solid curves tipped with arrows in Fig. 3.1. We computed only a sampling of periods, the period P_2 is observed to be continuous in h; more secondary bifurcations exist between our sampling.

To compute our sampling of dimension breaking bifurcations, we begin by guessing a large period at small amplitude. The small amplitude wave profiles at different periods are similar, and serve as a good initial guesses for nearby periods; the small amplitude case is numerically more forgiving with respect to poor guesses in P_2. An example of a fully three-dimensional wave at small amplitude, with large transverse period, is in Fig. 3.3. The planar wave from which Fig. 3.3 bifurcates is a classic Wilton ripple—in the small amplitude limit the wave resonates with its second harmonic, see [31,32]. After a single three-dimensional wave is found using (3.2), we use numerical continuation (in $\partial_\beta x_3$ at a point) to compute branches of three-dimensional waves.

To compute three-dimensional traveling waves which bifurcate from larger amplitudes, we use the numerical continuation to follow the period dependence on amplitude, $P_2 = P_2(h)$. That is, we use the period from one amplitude dimension breaking bifurcation as a starting point to search for the period of the next larger amplitude dimension breaking bifurcation. At all amplitudes we use the ansatz (3.2) for the displacement and vortex sheet strength of the first fully three-dimensional wave on a branch.

The guess (3.2) is ad-hoc, not based on formal asymptotics. We would prefer to have an explicit formula for waves which are weakly varying in the transverse direction, as in [33]; however, we believe such a solution is impossible to find, as it would require solving a linear non-constant coefficient PDE whose coefficients are only known numerically. The absence of such an asymptotic formula results in regions of parameter space where our initial guess (3.2) is not good enough to compute the dimension breaking bifurcations. That being said, we were able to compute dimension breaking along the entire branch of planar traveling waves in many configurations. One such configuration is depicted in Fig. 3.1, in which we compute dimension breaking bifurcations from a planar wave with $\sigma = 1/8$.

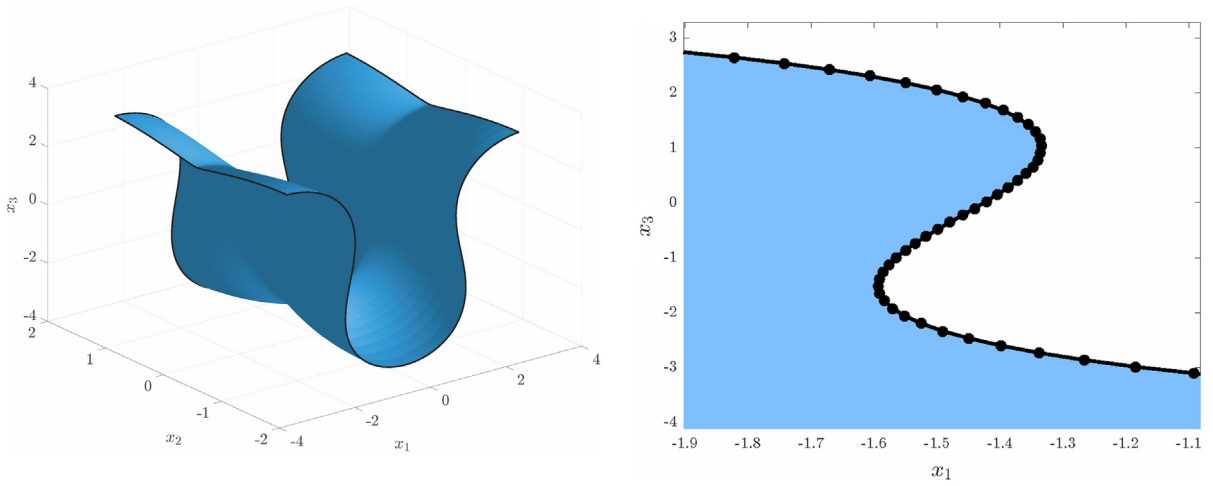

Fig. 3.4. An overturned fully three-dimensional traveling wave solution to (2.6), using the small-scale approximation to the Birkhoff–Rott integral. This wave was computed with At $= 1$, $\tau = 2$, $g = -0.2$, with $M_a = 128$ and $M_b = 32$. In the left panel is the three-dimensional surface, in the right panel is a close-up of a slice at $y = -\pi/2$. In the close-up on the right, the grid-points are marked with solid circles.

Generally we computed only small departures from the planar traveling waves, i.e. the local bifurcation structure. We did observe a case where the global bifurcation was also a small departure from planar. In the left panel of Fig. 3.1, observe the second and third to largest reported dimension-breaking bifurcations merge. These two bifurcations thus form the "return to trivial" global bifurcation. This phenomenon occurs in the two-dimensional setting as well, and is described in case (e) of the global bifurcation theorem of [34] and was numerically computed in [25].

In one space dimension there are two qualitatively different types of overturned traveling water waves. The first resemble the Crapper's wave, see the left panel of Fig. 1.1, which limits on an enclosed bubble and has large curvature in the neighborhood of this bubble. The second resembles the waves computed by Meiron and Saffman [23] and are more regular, see the right panel of Fig. 1.1. Numerically, the latter requires many fewer points to resolve; the planar wave has Fourier modes decaying to machine precision right at wave number $k = 32$ (corresponding to $M_a = 64$). In this work, we compute dimension breaking bifurcations near planar waves at two Bond numbers $\sigma = \frac{g}{k^2\tau}$, here k is the typical wave number of the planar wave based on its longitudinal period. The planar waves with $\sigma = 1/8$ resemble that of Crapper. The planar waves with $\sigma = -1/10$ resemble the waves of Meiron and Saffman.

An example of an overturned three-dimensional traveling wave is depicted in Fig. 3.4. This wave was computed via dimension breaking numerical continuation from a planar wave $\sigma = -1/10$. In this configuration the overturned planar wave is very regular (see the right panel of Fig. 1.1). Three-dimensional traveling waves were also computed via dimension breaking numerical continuation from planar waves with $\sigma = 1/8$. In the latter configuration we computed a number of dimension-breaking bifurcations, see Fig. 3.1. The waves computed in this figure all have interfaces which are functions of the horizontal Cartesian coordinates. In this case the overturned waves require significantly more points to resolve, and we were only able to resolve waves whose interfaces did not overturn.

Although we believe that there are fully three-dimensional overturned traveling waves at generic Bond numbers, bifurcations from waves with narrow bubbles (i.e. Crapper-like) require too many points for our current capabilities. Numerically we see evidence that overturned traveling waves exist in this setting, but we are only able to compute their under-resolved approximations. We are currently pursuing a study of overturned three-dimensional traveling waves in this more expensive case, as well as computing full Birkhoff–Rott integral, rather than its small scale approximation, using the Air Force Research Laboratory's supercomputing resource center [35].

4. Conclusion

Fully three-dimensional overhanging traveling waves are computed in the vortex sheet equations for water waves with surface tension. The small-scale approximation is used in the Birkhoff–Rott integral for the velocity field. A traveling wave ansatz for parameterized surfaces is presented. Large amplitude overhanging waves are computed via dimension-breaking continuation from planar traveling waves. Future research directions include computing these waves with the full Birkhoff–Rott integral, instead of the small scale approximation. Also desirable would be parameter space explorations, computing overturned traveling waves with fine structure, as would be the case for three-dimensional bifurcations from Crapper's wave. It is also natural to question as to whether any of these waves are stable to perturbations, and should they be unstable, how instabilities manifest in the time-dependent problem.

Acknowledgment

This work was partially supported by a grant from the Simons Foundation (#313852 to Benjamin Akers).

References

[1] D.M. Ambrose, M. Siegel, S. Tlupova, A small-scale decomposition for 3D boundary integral computations with surface tension, J. Comput. Phys. 247 (2013) 168–191.
[2] S.T. Grilli, P. Guyenne, F. Dias, A fully non-linear model for three-dimensional overturning waves over an arbitrary bottom, Internat. J. Numer. Methods Fluids 35 (7) (2001) 829–867.
[3] P. Lubin, S. Vincent, S. Abadie, J.-P. Caltagirone, Three-dimensional large eddy simulation of air entrainment under plunging breaking waves, Coast. Eng. 53 (8) (2006) 631–655.
[4] M. Xue, H. Xü, Y. Liu, D.K.P. Yue, Computations of fully nonlinear three-dimensional wave–wave and wave–body interactions. part 1. dynamics of steep three-dimensional waves, J. Fluid Mech. 438 (2001) 11–39.
[5] C. Fochesato, F. Dias, A fast method for nonlinear three-dimensional free-surface waves, in: Proceedings of the Royal Society of London A: Mathematical, Physical and Engineering Sciences, Volume 462, The Royal Society, 2006, pp. 2715–2735.
[6] T.Y. Hou, P. Zhang, Convergence of a boundary integral method for 3-d water waves, Discrete Contin. Dyn. Syst. Ser. B 2 (1) (2002) 1–34.
[7] A.L. New, P. McIver, D.H. Peregrine, Computations of overturning waves, J. Fluid Mech. 150 (1) (1985) 233–251.
[8] S.T. Grilli, F. Dias, P. Guyenne, C. Fochesato, F. Enet, Progress in fully nonlinear potential flow modeling of 3D extreme ocean waves, in: Advances in Numerical Simulation of Nonlinear Water Waves, 2010, pp. 75–128.
[9] D.I. Meiron, P.G. Saffman, H.C. Yuen, Calculation of steady three-dimensional deep-water waves, J. Fluid Mech. 124 (1982) 109–121.
[10] A.J. Roberts, Highly nonlinear short-crested water waves, J. Fluid Mech. 135 (1983) 301–321.
[11] C.H. Rycroft, J. Wilkening, Computation of three-dimensional standing water waves, J. Comput. Phys. 255 (2013) 612–638.
[12] D.P. Nicholls, F. Reitich, Stable, high-order computation of traveling water waves in three dimensions, Eur. J. Mech. B Fluids 25 (4) (2006) 406–424.
[13] E.I. Parau, J.-M. Vanden-Broeck, M.J. Cooker, Nonlinear three-dimensional gravity–capillary solitary waves, J. Fluid Mech. 536 (2005) 99–105.
[14] P.A. Milewski, Z. Wang, Transversally periodic solitary gravity–capillary waves, in: Proc. R. Soc. A, Volume 470, The Royal Society, 2014, p. 20130537.
[15] J.-M. Vanden-Broeck, T. Miloh, B. Spivack, Axisymmetric capillary waves, Wave Motion 27 (3) (1998) 245–256.
[16] Scott Grandison, Jean-Marc Vanden-Broeck, Demetrios T. Papageorgiou, Touvia Miloh, Boaz Spivak, Axisymmetric waves in electrohydrodynamic flows, J. Engrg. Math. 62 (2) (2008) 133–148.
[17] Tobias Osborne, Lawrence K. Forbes, Large amplitude axisymmetric capillary waves, in: IUTAM Symposium on Free Surface Flows, Springer, 2001, pp. 221–228.
[18] B. Akers, D.M. Ambrose, J.D. Wright, Traveling waves from the arclength parameterization: Vortex sheets with surface tension, Interfaces Free Bound. 15 (2013) 359–380.
[19] F. Dias, T.J. Bridges, The numerical computation of freely propagating time-dependent irrotational water waves, Fluid Dynam. Res. 38 (12) (2006) 803–830.
[20] T.Y. Hou, P. Hu, G.and Zhang, Singularity formation in three-dimensional vortex sheets, Phys. Fluids (1994-present) 15 (1) (2003) 147–172.
[21] D.M. Ambrose, M. Siegel, A non-stiff boundary integral method for 3D porous media flow with surface tension, Math. Comput. Simulation 82 (6) (2012) 968–983.
[22] G.D. Crapper, An exact solution for progressive capillary waves of arbitrary amplitude, J. Fluid Mech. 2 (06) (1957) 532–540.
[23] D.I. Meiron, P.G. Saffman, Overhanging interfacial gravity waves of large amplitude, J. Fluid Mech. 129 (1983) 213–218.
[24] B.F. Akers, D.M. Ambrose, J.D. Wright, Gravity perturbed crapper waves, Proc. R. Soc. Lond. Ser. A 470 (2161) (2014).
[25] B.F. Akers, D.M. Ambrose, K. Pond, J.D. Wright, Overturned internal capillary–gravity waves, Eur. J. Mech. B Fluids (2016).
[26] J. Beale, A convergent boundary integral method for three-dimensional water waves, Math. Comp. 70 (235) (2001) 977–1029.
[27] B. Akers, P.A. Milewski, A model equation for wavepacket solitary waves arising from capillary–gravity flows, Stud. Appl. Math. 122 (3) (2009) 249–274.
[28] J.-M. Vanden-Broeck, F. Dias, Gravity-capillary solitary waves in water of infinite depth and related free-surface flows, J. Fluid Mech. 240 (1992) 549–557.
[29] C.G. Broyden, A class of methods for solving nonlinear simultaneous equations, Math. Comp. 19 (1965) 577–593.
[30] H. Cheng, L. Greengard, V. Rokhlin, A fast adaptive multipole algorithm in three dimensions, J. Comput. Phys. 155 (2) (1999) 468–498.
[31] J.R. Wilton, On ripples, Phil. Mag. 29 (1915) 173.
[32] B.F. Akers, W. Gao, Wilton ripples in weakly nonlinear model equations, Commun. Math. Sci. 10 (3) (2012) 1015–1024.
[33] M.D. Groves, M. Haragus, S.M. Sun, A dimension–breaking phenomenon in the theory of steady gravity–capillary water waves, Philos. Trans. Roy. Soc. London Ser. A 360 (1799) (2002) 2189–2243.
[34] D.M. Ambrose, W.A. Strauss, J.D. Wright, Global bifurcation theory for periodic traveling interfacial gravity-capillary waves, Ann. Inst. H. Poincaré Anal. Non Linéaire 33 (4) (2016) 1081–1101.
[35] Air Force Research Laboratory (AFRL). U.S. Air Force Research Laboratory DoD Supercomputing Resource Center (AFRL DSRC), 2015.